JACS
JOURNAL OF THE AMERICAN CHEMICAL SOCIETY
Article
pubs.acs.org/JACS

Modulation of In-Membrane Receptor Clustering upon Binding of Multivalent Ligands

Anna Grochmal,[†] Elena Ferrero,[†] Lilia Milanesi,[‡] and Salvador Tomas*[,†]

[†]Institute of Structural and Molecular Biology and Department of Biological Sciences, School of Science, Birkbeck University of London, Malet Street, London WC1E 7HX, U.K.

[‡]School of Biological and Chemical Sciences, Queen Mary, University of London, Mile End Road, London E1 4NS, U.K.

Supporting Information

ABSTRACT: In living cells and biomimetic systems alike, multivalent ligands in solution can induce clustering of membrane receptors. The link between the receptor clustering and the ligand binding remains, however, poorly defined. Using minimalist divalent ligands, we develop a model that allows quantifying the modulation of receptor clustering by binding of ligands with any number of binding sites. The ligands, with weak binding affinity for the receptor and with binding sites held together by flexible linkers, lead to nearly quantitative clustering upon binding in a wide range of experimental conditions, showing that efficient modulation of receptor clustering does not require pre-organization or large binding affinities per binding site. Simulations show that, in the presence of ligands with five or more binding sites, an on/off clustering response follows a very small change in receptor density in the membrane, which is consistent with the highly cooperative behavior of multivalent biomolecular systems.

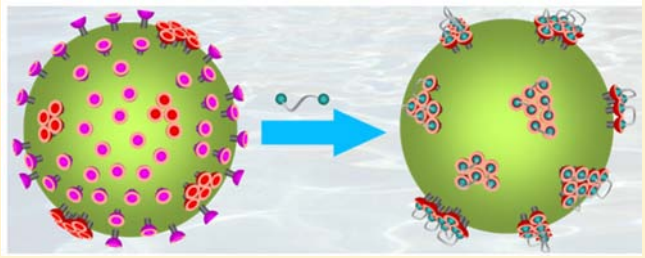

1. INTRODUCTION

The cell membrane is a very complex construct that defines the cell and regulates the contact of the cell with the environment.[1] Minute changes in the cell environment are picked up by the cell membrane, generating the appropriate response within the cell. In most cases, the response requires changes in the organization of membrane components. For example, signal transduction, which is at the heart of both the immunological response and neurotransmission, involves the formation of clusters of specialized membrane-associated proteins, which can be initiated by the presence in the medium of the appropriate chemical species.[2−8] Clearly, understanding the mechanism of the clustering of membrane-associated molecules, and what role their binding to extra-membrane molecules plays in the clustering process, is essential in order to understand how the cell membrane works at the molecular level.

Minimalist chemical systems have been developed that exploit the ability of membrane-embedded receptors to form clusters, and have found applications in sensing and catalysis.[9−16] Minimalist systems are also useful to analyze the binding of in-solution molecules to surface-confined receptors in the absence of biomolecular complexity. For example, efforts have led to the development of simple and elegant analytical models that allow quantifying the binding of multivalent ligands to a surface covered with closely packed receptors,[17] and the relationship between intra-membrane (leading to receptor clustering) and inter-membrane (leading to liposome aggregation) binding of multivalent ligands in a lipid membrane.[18] The close relationship between receptor clustering and ligand binding has also been highlighted. Thus, the formation and destruction of clusters of receptors upon binding of the ligand has been described.[19−23] Conversely, it has been reported that the receptor clusters may show a different affinity for a multivalent ligand and lead even to membrane adhesion.[24−27] In these works however the focus is in the description of the phenomenon, and no attempt is made to quantify the mutual modulation between the binding of the ligand and clustering of the receptor.

Recently, we developed a model that allowed us to quantify the clustering−disperse equilibrium of a membrane-embedded receptor and evaluate what effect the binding of a ligand has on this equilibrium.[28] The model allowed us to demonstrate that the binding to a ligand in solution and the clustering of a membrane-embedded receptor are closely related processes that modulate each other, even in the absence of a clear multivalence effect or a conformational change in the receptor. Clearly, monovalent ligands modulate the clustering of the receptor because the binding of the ligand modifies the stability of the clustered form. A multivalent ligand should be able to enhance the receptor cluster stability by binding preferably to the pre-existing cluster and by recruiting disperse receptors. Crucially, it has been observed that affinity increases at higher receptor densities in the membrane.[29−33] In this work we use a minimalist chemical system composed of liposomes, an uncomplicated synthetic receptor, and a family of minimal

Received: May 9, 2013
Published: June 13, 2013

multivalent (i.e., divalent) ligands with the aim of analyzing in detail the interplay between receptor clustering and multivalent ligand binding.

2. RESULTS AND DISCUSSION

2.1. Design and Synthesis of the Model System. Membrane-anchored receptor **1** has been previously used in the study of the modulation of clustering by the binding of monovalent ligands. The Zn-porphyrin headgroup fulfills the role of binding site, specific for basic N-bearing ligands, and also as reporting moiety on account of its characteristic changes in the UV−vis absorption and fluorescence spectra upon clustering and ligand binding.[28] **1** has been shown to form clusters while embedded in the membrane, the stability of which is described by the clustering constant:

$$K_{DC} = \frac{[C]R_L}{[D]} \quad (1)$$

where C is any cluster of **1** containing two or more molecules, D is the dispersed form of **1**, and R_L is the ratio [Lipid]/[**1**]. Changes in the absorbance of **1** with R_L are used to determine K_{DC}, which is 13.6. This result means that at R_L = 13.6 (i.e., 6.8% receptor loading), 50% of embedded **1** is found in the cluster C form and 50% in the dispersed D form (see Supplementary Figure 2).

Imidazole derivatives **L1**, **L2**, **L3**, and **L4** (Figure 1) are used as model ligands, as they display a moderate binding affinity to

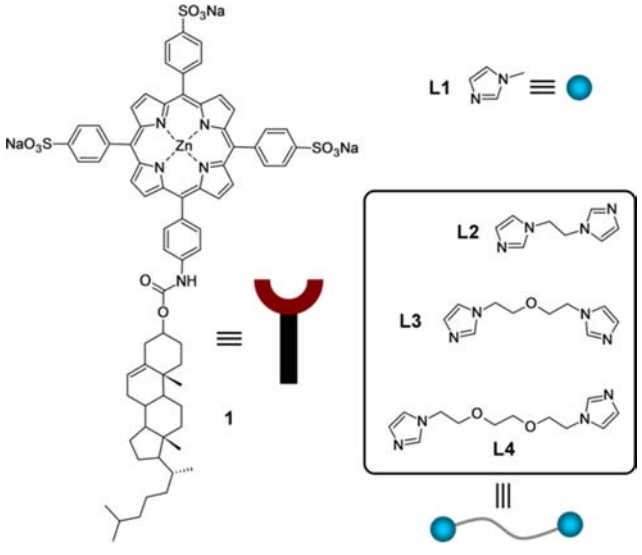

Figure 1. Chemical structure and cartoon representation of the receptor **1** and the ligands **L1**−**L4**.

Zn metaloporphyrins which is easy to measure.[34] **L1** is used as reference monovalent ligand. **L2**, **L3**, and **L4** are divalent, the difference among them being the linker length. This design feature was introduced in order to evaluate the relative importance of linker flexibility and binding site separation distance on the overall clustering modulation effect (see experimental methods in Supporting Information for synthesis of ligands **L2**−**L4**).

2.2. Monovalent Ligand Binding. As previously reported,[28] the interplay between binding of a monovalent ligand to a membrane-embedded receptor and the clustering of the receptor can be analyzed using a binding-clustering thermodynamic cycle (Figure 2a). The binding affinities for the C and D forms of the receptor, K_C and K_D, are defined as:

$$K_C = \frac{[C\cdot\mathbf{L1}]}{[C][\mathbf{L1}]} \quad (2)$$

$$K_D = \frac{[D\cdot\mathbf{L1}]}{[D][\mathbf{L1}]} \quad (3)$$

which together with K_{DC} and K_{DCL} define the thermodynamic cycle (Figure 2a). Fitting the changes of the UV spectrum of **1** at different R_L values and concentration of **L1** to this binding−clustering model allows determining all the equilibrium constants. K_{DC} is entered as a fixed parameter, determined from the fitting of the spectroscopic data in the absence of the ligand. K_{DCL} is obtained from the completion of the thermodynamic cycle ($K_{DCL} = K_{DC}K_C/K_D$) (Table 1). The data fitting allows also to extrapolate the spectra for the pure species, C, D, C·**L1**, and D·**L1**, which are consistent with the expected changes upon binding and clustering (Figure 2b,c).[28]

The modulation factor (M_f) for the monovalent ligand **L1** quantifies how strongly the clustering is modulated by the binding (and vice versa), and it is defined as:

$$M_f = \frac{K_C}{K_D} \quad (4)$$

or

$$M_f = \frac{K_{DCL}}{K_{DC}} \quad (5)$$

which results in a M_f of 3.2 (Table 1). This result means that, for a given R_L (i.e., a particular receptor density in the membrane), the relative amount of the cluster form C increases 3.2 times upon binding of the ligand **L1**. Conversely, upon clustering, the amount of complex increases 3.2 times at a given concentration of ligand **L1**. This result is consistent with results reported earlier for a number of similar monovalent ligands.[28] In the absence of a clear multivalent effect, it can be attributed to the different environments in the C and D forms of the receptor (i.e., more or less hydrophobic) from the point of view of the binding enhancement, or a better packing of the complex in relation to the free receptor, from the point of view of the clustering enhancement.

2.3. Divalent Ligand Binding. For ligands **L2**−**L4** there is the possibility that the binding of the second site may lead to vesicle adhesion, i.e., that the second binding event be inter- rather than intra-vesicular. Inter-vesicular adhesion is typically accompanied by an increase in the turbidity and scattering of the sample.[18,21] Both turbidity and sample scattering are, however, insensitive to ligand addition at moderate R_L (up to 250) for any ligand. Therefore, in these conditions, all multivalent binding is assumed to take place intravesicularly.

For all the ligands the binding site is an alkylimidazole. It is reasonable to assume that the microscopic binding constants (i.e., the binding constants per binding site) that lead to the complexes D·L and C·L have the same value for all the ligands. If this assumption is correct the measured macroscopic binding constants for the divalent ligands **L2**−**L4** are expected to be twice of that for the monovalent ligand **L1**, on account of the presence of twice as many identical binding sites in ligands **L2**−**L4**. This is experimentally shown to be the case: the value of the apparent binding constant, K_{ap}, at large R_L values (i.e., when most of **1** is in the D form and $K_{ap} \approx K_D$) is, within the error,

dx.doi.org/10.1021/ja404428u | J. Am. Chem. Soc. 2013, 135, 10172−10177

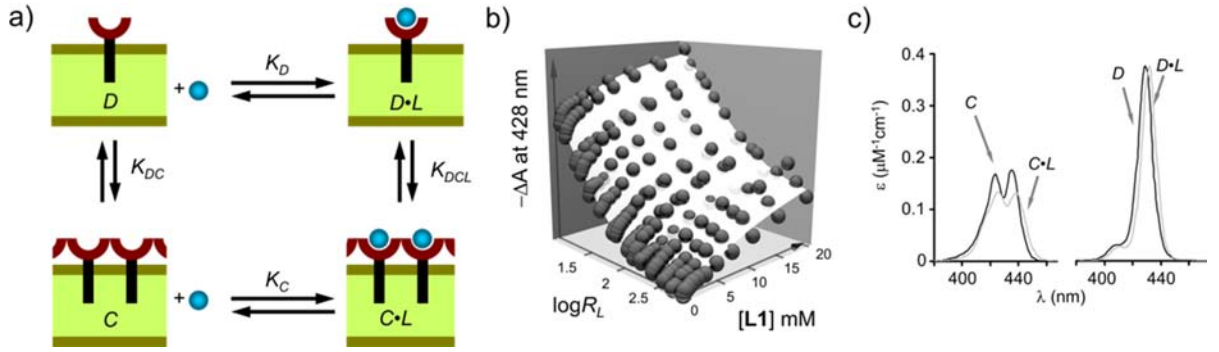

Figure 2. (a) Cartoon representation of the ligand binding−receptor clustering thermodynamic cycle for monovalent ligand **L1**. (b) Changes in absorbance ($-\Delta A$) at 428 nm with changes in log R_L and concentration of **L1** (dark spheres). The white surface is the best fit to the clustering−binding model using the program Specfit 3.0 (see Supporting Information for details). (c) Soret band region of UV−vis spectra for the pure species (with ligand **L1**) derived from the global fitting procedure, using the program SPECFIT 3.0 (see Supporting Information for details).

Table 1. Binding and Clustering Parameters for L1[a]

K_C (M^{-1})	K_D (M^{-1})	K_{DC}	K_{DCL}	M_f
130 ± 10	41 ± 4.3	13.6 ± 1.5	44 ± 4.3	3.2 ± 0.65

[a]The error quoted is twice the standard deviation.

the same for ligands **L2**−**L4** and twice as much the value of K_{ap} for ligand **L1** (Supplementary Table 1). Therefore, K_D(divalent) is twice K_D(monovalent) (Figure 3).

The binding of the divalent ligands to the cluster C form of the receptor can yield two kinds of complexes: C·L and C_2·L (Figure 3). The equilibrium constants for the formation of C·L from C and L is K_{C1}, and it is assumed to have a value that is twice the binding constant for the binding of **L1** to C, K_C (see above). The equilibrium constant that relates C·L and C_2·L, K_{C2} can be expressed as a function of the concentrations of C, C·L, and C_2·L:

$$K_{C2} = \frac{[C_2{\cdot}L][\mathbf{1}]}{[C{\cdot}L][C]} \qquad (6)$$

where [**1**] is the total concentration of the receptor (see Supporting Information for the derivation of eq 6).

The relationship between all the individual species (D, C, D·L, C·L, and C_2·L) can be written in the form of an extended thermodynamic cycle, where all the equilibrium constants are derived from the four constants K_{DC}, K_D, K_{C1}, and K_{C2} (see Supplementary Figures 3 and 4 and related discussion in the Supporting Information). Thus, by determining these constants all the concentrations of the species can be determined for any particular set of initial conditions. The UV titration data of embedded receptor **1** with ligands **L2**−**L4** at different R_L values was fitted to a model that takes into account the formation of five colored species (D, C, D·L, C·L, and C_2·L) related through four independent equilibrium constants, K_{DC}, K_D, K_{C1}, and K_{C2} (Figure 3a). Of these, K_{DC}, K_D, and K_{C1} are determined by the fitting of the spectroscopic data in the absence of ligand (K_{DC}) and by the fitting of the data from titrations with ligand **L1**. The fitting of the data from titrations with ligand **L1** yields also the spectra of the species D, C, D·L, and C·L (Figure 2c), which are entered in the fitting of **L2**−**L4** as known parameters. Thus, the only unknown parameters are K_{C2} (Table 2) and the extinction coefficient (i.e., the UV spectra) of C_2·L. The fitting is remarkably good for all the ligands, showing that the

Table 2. Binding and Clustering Parameters for Ligands L2−L4[a]

	L2	L3	L4
K_{C2}	6.3 ± 0.72	12 ± 1.5	70 ± 8.1
EM (M)	0.098 ± 0.010	0.19 ± 0.022	1.1 ± 0.12

[a]The error quoted is twice the standard deviation.

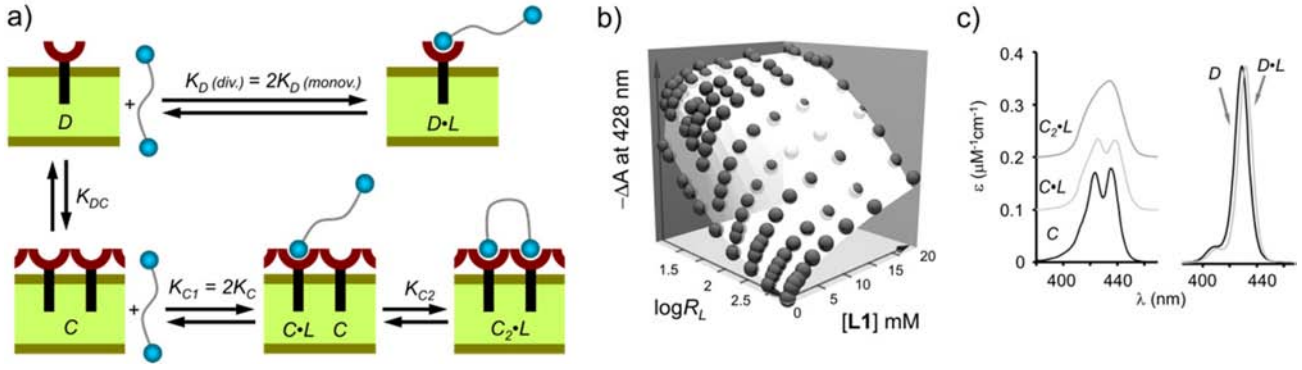

Figure 3. (a) Schematic representation of the clustering-binding equilibria defined by the four independent equilibrium constants K_D, K_{DC}, K_{C1}, and K_{C2} (see Supplementary Figure 4 for full thermodynamic cycle). (b) Changes in absorbance ($-\Delta A$) at 428 nm with changes in log R_L and concentration of **L4** (dark spheres). The white surface is the best fit to the clustering−binding model using the program SPECFIT 3.0 (see Supporting Information for details). (c) Soret band region of UV−vis spectra for the pure species (with ligand **L4**). Only C_2·L spectrum is obtained from the fitting of **L4** data. C, C·L, D, and D·L spectra are obtained from the fitting of **L1** data and are displayed here for comparison purposes.

dx.doi.org/10.1021/ja404428u | J. Am. Chem. Soc. 2013, 135, 10172−10177

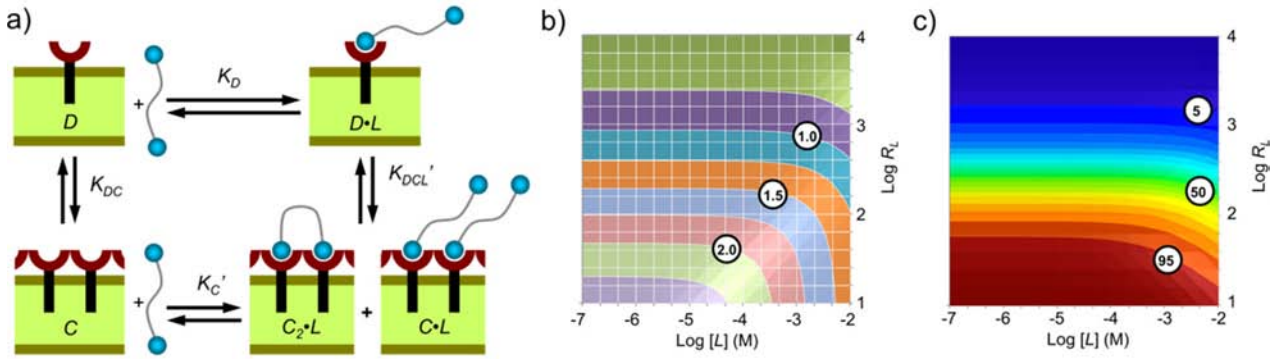

Figure 4. (a) Simplified form of the thermodynamic binding−clustering cycle for divalent ligands. (b) Contour plot of the variation of the log M_f for the binding of **L4** to membrane-embedded **1** at different concentrations of **L4** and increase of R_L (concentration of **1** = 2 μM). Each color represents an increase of log M_f of 0.25 unit. (c) Percentage of complex in the cluster form at different R_L and concentrations of ligand **L4**. Each color represents an increase of 5% (concentration of **1** = 2 μM).

assumptions made for K_D and K_{C1} are reasonable (Figure 3b and Supplementary Figure 2). The extrapolated UV spectrum for the Soret band region is also consistent with the expected spectrum of a ligand-bound clustered receptor: broad and red-shifted in relation with the ligand-free species (Figure 3c and Supplementary Figure 2).

Our aim is to establish how strongly binding and clustering modulate each other, regardless of the precise stoichiometry of the receptor−ligand complex formed. This modulation is graphically illustrated in a simplified thermodynamic cycle that relates four species through the equilibrium constants K_{DC}, K_D, K_{DCL}', and K_C' (Figure 4a). K_C' and K_{DCL}' are the apparent equilibrium constants that take different values at different concentrations of ligand and R_L values, but can be determined for any set of initial conditions by using the values of K_{C1}, K_{C2}, K_D, and K_{DC} determined from the fitting of the data. K_C' can be written as:

$$K_C' = \frac{[C{\cdot}L] + 2[C_2{\cdot}L]}{[C][L]} \tag{7}$$

Knowing K_C', it is possible to determine the modulation factor M_f for ligands **L2**−**L4**, which is defined as:

$$M_f = \frac{K_C'}{K_D} \tag{8}$$

or

$$M_f = \frac{K_{DCL}'}{K_{DC}} \tag{9}$$

Like K_C' and K_{DCL}', M_f varies with both the concentration of ligand and R_L. Clearly, the formation of cluster complex $C_2{\cdot}L$ is favored by the presence of free C. Therefore, M_f will be larger in conditions when [C] is larger, i.e., at low ligand concentration and low R_L values.

In all cases, M_f is larger for the divalent **L2**−**L4** ligands than the monovalent **L1** in a wide range of experimental conditions (Figure 4b and Supplementary Figure 5). This behavior is expected from a ligand with multiple binding sites, where the additional complex $C_2{\cdot}L$ contributes to enhance the stability of the cluster. Unexpectedly, the results also show that the ligand with the longest and more flexible linker, **L4**, displays the largest M_f. In the case of **L4**, M_f is larger than 100 in a wide range of experimental conditions (Figure 4b). In practical terms, this means that binding of the ligand leads to near-quantitative clustering of the receptor in these conditions (Figure 4c).

2.4. Effective Molarity. The effective molarity, EM, is typically seen as the local concentration of complementary binding sites in a complex held by multiple interactions. EM is therefore a measure of how efficient multivalency or chelate effect is in increasing the stability of a complex. In our system, the clustered form C can be considered as a multivalent receptor. Thus, the formation constant of $C_2{\cdot}L$ from C·L and C, K_{C2}, can be written as a function of EM as follows:

$$K_{C2} = 0.5K_C\mathrm{EM} \tag{10}$$

where 0.5 is the statistical correction factor. The calculated values of EM (i.e., 0.1−1.1 M, Table 2) are within the expected value for systems involving ligands of similar size.[35] For our divalent ligands, EM increases with the length and the flexibility of the linker, which is a trend that is the opposite to the one normally observed in systems where the second binding event leads to ring closure.[35] It is worth noting that $C_2{\cdot}L$ can be formed by the additional binding of C·L to any surrounding free C. Molecular modeling suggest that ligands **L2** and **L3** can only reach the nearest neighbor (i.e., up to a maximum of six binding sites in a close-packed cluster, Supplementary Figure 6). On the other hand for **L4** the second binding site may reach up to 18 neighboring receptor binding sites. This difference would result in a 3-fold increase in the EM for **L4** relative to **L2** and **L3**, which accounts, at least partly, for the trend in EM values between the divalent ligands.

There is a direct relationship between EM and M_f that can be mathematically expressed as (see SI for details):

$$M_f(\text{divalent}) = M_f(\text{monovalent})\left(1 + K_C\mathrm{EM}\frac{[C]}{[\mathbf{1}]}\right) \tag{11}$$

Equation 11 clearly shows that the ligand binding chelate effect, quantified as EM, is transferred to the membrane−water interface, where the conditions of relatively high local concentration make a relatively weak cooperative effect more efficient. Equation 11 has the drawback that requires [C] to be determined at each point of the titration in order to calculate M_f. A version of eq 11 can be drawn for the modulation factor of the binding of the first aliquot of the ligand, which depends only on the initial conditions of the experiment (see Supporting Information for details):

dx.doi.org/10.1021/ja404428u | J. Am. Chem. Soc. 2013, 135, 10172−10177

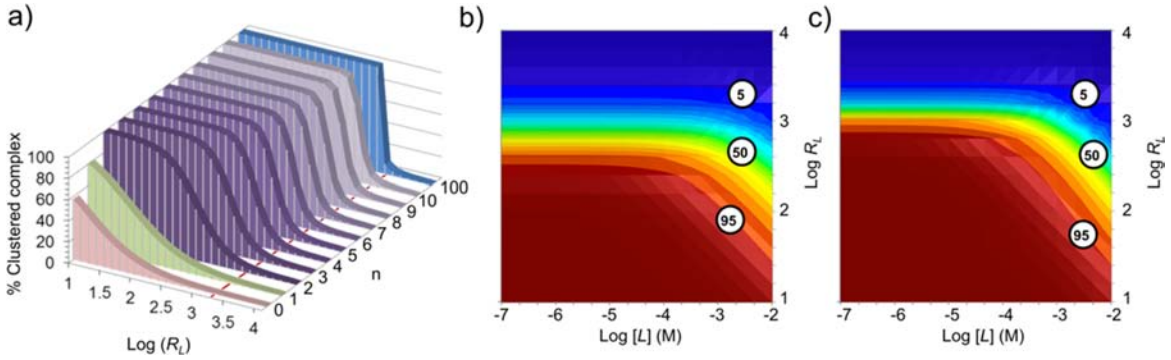

Figure 5. (a) Percentage of complex clustered upon binding to receptor **1** of the first ligand aliquot for derivatives of ligand **L4** with increasing number of binding sites. The percentages of cluster for the free receptor (n = 0) and complex with a monovalent ligand (n = 1) are shown for comparison. The red line marks the limit in R_L (ca. 1900) above which no cluster response follows ligand binding. (b) Percentage of complex clustered upon binding to receptor **1** of a derivative of ligand **L4** with four binding sites. Each shade represents an increase of 5%. (c). Percentage of complex clustered upon binding to receptor **1**of a derivative of ligand **L4** with eight binding sites. Each shade represents an increase of 5%. The concentration of **1** is 2 μM in all cases.

$$M_f(\text{divalent,initial}) = M_f(\text{monovalent})\left(1 + K_C\text{EM}\frac{K_{DC}}{K_{DC} + R_L}\right) \quad (12)$$

Equation 12 shows that the M_f is enhanced by large K_C, EM, and K_{DC} values, and it is reduced by high R_L (equivalent to low receptor density). However, a large response in the organization of membrane-embedded **1** does not requires very large K_C, EM, and K_{DC} values. As we have already seen, our ligands are able to elicit a strong clustering response upon binding (Figure 4b,c and, Supplementary Figure 5). The efficiency in driving the cluster for a multivalent ligand with intrinsic low K_C and EM is better illustrated considering a hypothetic ligand with n binding sites.

2.5. Clustering-Binding M_f for the Binding of n-Valent Ligands. It can be shown that for a multivalent ligand with n independent identical binding sites (i.e., with identical EM and binding constant K_C for each site), the modulation factor M_f can be written as (see Supporting Information for details):

$$M_f(n\text{-valent}) = M_f(\text{monovalent})\left(1 + \sum_{i=2}^{i=n}\left(K_C\text{EM}\frac{[C]}{[\mathbf{1}]}\right)^{i-1}\right) \quad (13)$$

$$M_f(n\text{-valent,initial}) = M_f(\text{monovalent})\left(1 + \sum_{i=2}^{i=n}\left(K_C\text{EM}\frac{K_{DC}}{K_{DC} + R_L}\right)^{i-1}\right) \quad (14)$$

Equations 13 and 14 can be applied to simulate the clustering modulation factor of any hypothetic ligand containing n identical binding sites if the values of K_C, K_{DC}, and EM are known. For example, for a ligand with the same K_C, K_D, and EM values of **L4** for receptor **1**, the simulation shows that clustering is quantitative upon ligand binding for R_L as high as 500 (i.e., receptor densities as low as 0.2%) with n as low as 4 (Figure 5a,b). From eq 14, it is possible to predict the maximum R_L (i.e., minimum receptor density) required for a multivalent ligand to be able to induce the clustering of the receptor, i.e.,

$$R_L < K_C\text{EM}K_{DC} - K_{DC} \quad (15)$$

Thus, for **L4** derivatives binding to **1**, R_L must be less than ca. 1900 (i.e., ligand density larger than 0.053%). This is graphically shown in Figure 5. Strikingly, for n > 5, the clustering response upon ligand binding becomes strongly sensitive to very small changes in receptor density. Thus, for n = 8, a receptor density of 0.04% (R_L = 2500) is hardly affected by the binding of the ligand, while a density of 0.11% (R_L = 910) results in >98% of clustering upon ligand binding (Figure 5a,c). For very large n, the difference is even more notable. For example, for n = 100, changing the density from 0.05 to 0.06% (i.e., R_L from 2000 to 1700) leads to quantitative clustering (i.e., >99.9%) (Figure 5a).

3. CONCLUSIONS

In summary, in this work we quantify how the clustering of a membrane-embedded receptor is modulated by the binding of a divalent ligand in solution. The modulation of clustering is attributed to the combination of two effects: first, the larger affinity of each binding site for the clustered form, as reflected by M_f(monovalent), and second, the effect of molarity EM for the formation of the complex C_2·L. Both effects are intrinsically weak; i.e., M_f (monovalent) is 3.2, and the EM is between 0.1 and 1 M. The implications are that for membrane-embedded receptors, the binding of flexible ligands with a low level of pre-organization or even low binding affinity per site can trigger an on/off behavior typical of biomolecular systems.[36] Simulations for n-valent ligands show that clustering response upon ligand binding becomes very sensitive to small variations of receptor density in the membrane for n values larger than 5. As a consequence, a small amount in the input signal variation (i.e., receptor density in the membrane) leads to an on/off output signal (clustering) from the system. The model allows also estimating the on/off switching point when the individual binding constants are known. The predictions of the model are therefore consistent with the attribution of the large cooperative effects typical of biomolecular systems to a multivalent chelate effect,[37] and may find applicability in the analysis of a number of cell membrane processes, including cell adhesion, which require both receptor clustering and multivalence to take effect. The analysis reported here offers also a useful tool for the design of responsive *de novo* systems based on cell-like compartments.

dx.doi.org/10.1021/ja404428u | J. Am. Chem. Soc. 2013, 135, 10172−10177

■ ASSOCIATED CONTENT

Supporting Information

Experimental methods (including synthesis of **L2**−**L4**, sample preparation, data processing, and titration experiments), **1** clustering and **L2** and **L3** titration data, molecular modeling calculations, detailed derivation of the equations, and detailed data fitting procedures. This material is available free of charge via the Internet at http://pubs.acs.org.

■ AUTHOR INFORMATION

Corresponding Author

s.tomas@bbk.ac.uk

Notes

The authors declare no competing financial interest.

■ ACKNOWLEDGMENTS

This work was funded by the Faculty of Sciences, Birkbeck, University of London. We thank C. A. Hunter for critical reading of the manuscript.

■ REFERENCES

(1) Luckey, M. *Membrane Structural Biology*; Cambridge University Press: Cambridge, UK, 2008.
(2) Grakoui, A.; Bromley, S. K.; Sumen, C.; Davis, M. M.; Shaw, A. S.; Allen, P. M.; Dustin, M. L. *Science* **1999**, *285*, 221.
(3) Renner, M.; Specht, C. G.; Triller, A. *Curr. Opin. Neurobiol.* **2008**, *18*, 532.
(4) Tolar, P.; Hanna, J.; Krueger, P. D.; Pierce, S. K. *Immunity* **2009**, *30*, 44.
(5) Munoz, P.; Mittelbrunn, M.; de la Fuente, H.; Perez-Martinez, M.; Garcia-Perez, A.; Ariza-Veguillas, A.; Malavasi, F.; Zubiaur, M.; Sanchez-Madrid, F.; Sanchol, J. *Blood* **2008**, *111*, 3653.
(6) Simons, K.; Toomre, D. *Nat. Rev. Mol. Cell Biol.* **2000**, *1*, 31.
(7) Allen, J. A.; Halverson-Tamboli, R. A.; Rasenick, M. M. *Nat. Rev. Neurosci.* **2007**, *8*, 128.
(8) Boniface, J. J.; Rabinowitz, J. D.; Wulfing, C.; Hampl, J.; Reich, Z.; Altman, J. D.; Kantor, R. M.; Beeson, C.; McConnell, H. M.; Davis, M. M. *Immunity* **1998**, *9*, 459.
(9) Banerjee, S.; Konig, B. *J. Am. Chem. Soc.* **2013**, *135*, 2967.
(10) Gruber, B.; Kataev, E.; Aschenbrenner, J.; Stadlbauer, S.; Konig, B. *J. Am. Chem. Soc.* **2011**, *133*, 20704.
(11) Mancin, F.; Scrimin, P.; Tecilla, P.; Tonellato, U. *Coord. Chem. Rev.* **2009**, *253*, 2150.
(12) Voskuhl, J.; Ravoo, B. J. *Chem. Soc. Rev.* **2009**, *38*, 495.
(13) Noble, G. T.; Craven, F. L.; Voglmeir, J.; Sardzik, R.; Flitsch, S. L.; Webb, S. J. *J. Am. Chem. Soc.* **2012**, *134*, 13010.
(14) Mahon, E.; Aastrup, T.; Barboiu, M. *Chem. Commun.* **2010**, *46*, 2441.
(15) Gruber, B.; Konig, B. *Chem.—Eur. J.* **2013**, *19*, 438.
(16) Barnard, A.; Smith, D. K. *Angew. Chem., Int. Ed.* **2012**, *51*, 6572.
(17) Huskens, J.; Mulder, A.; Auletta, T.; Nijhuis, C. A.; Ludden, M. J. W.; Reinhoudt, D. N. *J. Am. Chem. Soc.* **2004**, *126*, 6784.
(18) Wang, X.; Mart, R. J.; Webb, S. *J. Org. Biomol. Chem.* **2007**, *5*, 2498.
(19) Denisov, G.; Wanaski, S.; Luan, P.; Glaser, M.; McLaughlin, S. *Biophys. J.* **1998**, *74*, 731.
(20) Liem, K. P.; Noble, G. T.; Flitsch, S. L.; Webb, S. J. *Faraday Discuss.* **2010**, *145*, 219.
(21) Gruber, B.; Balk, S.; Stadlbauer, S.; Konig, B. *Angew. Chem., Int. Ed.* **2012**, *51*, 10060.
(22) Christian, D. A.; Tian, A. W.; Ellenbroek, W. G.; Levental, I.; Rajagopal, K.; Janmey, P. A.; Liu, A. J.; Baumgart, T.; Discher, D. E. *Nat. Mater.* **2009**, *8*, 843.
(23) Sasaki, D. Y.; Waggoner, T. A.; Last, J. A.; Alam, T. M. *Langmuir* **2002**, *18*, 3714.
(24) Noble, G. T.; Flitsch, S. L.; Liem, K. P.; Webb, S. *J. Org. Biomol. Chem.* **2009**, *7*, 5245.
(25) Gong, Y.; Ma, M.; Luo, Y.; Bong, D. *J. Am. Chem. Soc.* **2008**, *130*, 6196.
(26) Mart, R. J.; Liem, K. P.; Wang, X.; Webb, S. J. *J. Am. Chem. Soc.* **2006**, *128*, 14462.
(27) Meyenberg, K.; Lygina, A. S.; van den Bogaart, G.; Jahn, R.; Diederichsen, U. *Chem. Commun.* **2012**, *47*, 9405.
(28) Tomas, S.; Milanesi, L. *Nat. Chem.* **2010**, *2*, 1077.
(29) Thomas, G. B.; Rader, L. H.; Park, J.; Abezgauz, L.; Danino, D.; DeShong, P.; English, D. S. *J. Am. Chem. Soc.* **2009**, *131*, 5471.
(30) Jiang, H.; Smith, B. D. *Chem. Commun.* **2006**, 1407.
(31) Kauscher, U.; Ravoo, B. J. *Beilstein J. Org. Chem.* **2012**, *8*, 1543.
(32) Doyle, E. L.; Hunter, C. A.; Phillips, H. C.; Webb, S. J.; Williams, N. H. *J. Am. Chem. Soc.* **2003**, *125*, 4593.
(33) Jung, H.; Robison, A. D.; Cremer, P. S. *J. Struct. Biol.* **2009**, *168*, 90.
(34) Tomas, S.; Milanesi, L. *J. Am. Chem. Soc.* **2009**, *131*, 6618.
(35) Misuraca, M. C.; Grecu, T.; Freixa, Z.; Garavini, V.; Hunter, C. A.; van Leeuwen, P.; Segarra-Maset, M. D.; Turega, S. M. *J. Org. Chem.* **2011**, *76*, 2723.
(36) Martinez-Veracoechea, F. J.; Frenkel, D. *Proc. Natl. Acad. Sci. U.S.A.* **2011**, *108*, 10963.
(37) Hunter, C. A.; Anderson, H. L. *Angew. Chem., Int. Ed.* **2009**, *48*, 7488.